

Effective medium approximation and the complex optical properties of the inhomogeneous superconductor $\text{K}_{0.8}\text{Fe}_{2-y}\text{Se}_2$

C. C. Homes,* Z. J. Xu, J. S. Wen, and G. D. Gu
*Condensed Matter Physics and Materials Science Department,
Brookhaven National Laboratory, Upton, New York 11973, USA*
(Dated: August 27, 2021)

The in-plane optical properties of the inhomogeneous iron-chalcogenide superconductor $\text{K}_{0.8}\text{Fe}_{2-y}\text{Se}_2$ with a critical temperature $T_c = 31$ K have been modeled in the normal state using the Bruggeman effective medium approximation for metallic inclusions in an insulating matrix. The volume fraction for the inclusions is estimated to be $\simeq 10\%$; however, they appear to be highly distorted, suggesting a filamentary network of conducting regions joined through weak links. The value for the plasma frequency $\omega_{p,D}$ in the inclusions is much larger than the volume average, which when considered with the reasonably low values for the scattering rate $1/\tau_D$, suggests that the transport in the grains is always metallic. Estimates for the dc conductivity σ_{dc} and the superfluid density ρ_{s0} in the grains places the inclusions on the universal scaling line $\rho_{s0}/8 \simeq 4.4\sigma_{dc}T_c$ close to other homogeneous iron-based superconductors.

PACS numbers: 74.25.Gz, 74.70.-b, 74.81.-g, 63.20.-e

I. INTRODUCTION

The surprising discovery of superconductivity in the iron-pnictide and iron-chalcogenide compounds with relatively high critical temperatures (T_c 's) has generated a great deal of interest in these materials.¹ The minimal electronic structure is characterized by hole and electron pockets at the center and corners of the Brillouin zone, respectively.² It has been proposed that the scattering between the electron and hole pockets forms the basis of a spin-fluctuation pairing mechanism.³ For this reason, the discovery of superconductivity in $\text{K}_{0.8}\text{Fe}_{2-y}\text{Se}_2$ was of particular interest because the hole pocket in this material is absent,⁴⁻⁶ yet a relatively high $T_c \simeq 31$ K is observed,⁷ as opposed to the hole-doped analog KFe_2As_2 , which has a dramatically-reduced $T_c \simeq 3$ K.^{8,9} This suggests that the pairing mechanism may not be a settled issue in these materials.¹⁰ A further complication in understanding the physical properties of $\text{K}_{0.8}\text{Fe}_{2-y}\text{Se}_2$ arises from the growing body of evidence that suggests that this material is not homogeneous, but instead consists of non-magnetic metallic (superconducting) inclusions in a magnetic, insulating matrix.¹¹⁻²⁵ The optical properties of $\text{K}_{0.8}\text{Fe}_{2-y}\text{Se}_2$, and the related $\text{Rb}_2\text{Fe}_4\text{Se}_5$ material, have been investigated in some detail and also support the conclusion that these materials are inhomogeneous.²⁵⁻²⁸ The phase-separated nature of these materials complicates the optical determination of the complex dielectric function, which is by nature a volume-averaging technique. However, a recent study of $\text{K}_{0.8}\text{Fe}_{2-y}\text{Se}_2$ by Wang *et al.*²⁵ noted that the optical properties of this material could be described quite well using an effective medium theory for the dielectric function which consists of separate contributions from metallic inclusions embedded in an insulating matrix.²⁹⁻³²

Our original study of the optical properties of $\text{K}_{0.8}\text{Fe}_{2-y}\text{Se}_2$ noted that the normal and superconducting state properties both indicated that this material

was inhomogeneous, and that the superconductivity was due to Josephson coupling between the superconducting regions.²⁸ In view of the phase-separated nature of this material, the application of an effective medium theory to our optical data is a necessary next step in modeling the optical properties. In this work we apply the Bruggeman effective-medium approximation dielectric function³² to the normal-state optical properties of $\text{K}_{0.8}\text{Fe}_{2-y}\text{Se}_2$. The metallic inclusions appear to comprise about 10% of the total sample volume, resulting in a Drude plasma frequency that is significantly higher than the volume-averaged value²⁸ but is still much smaller than the values observed in other (homogeneous) iron-based superconductors,³³⁻⁴⁰ unless volume fractions of less than 1% are considered. Interestingly, and in agreement with another recent study of the optical properties of this material,²⁵ the EMA can not be applied to the data successfully without assuming that the inclusions are extremely distorted, suggesting the formation of filamentary conducting networks.^{21,41} The estimated superconducting plasma frequency of the inclusions is again much larger than the volume-averaged value, but still significantly smaller than the values determined in other iron-based superconductors. The volume-averaged values for the dc conductivity (measured just above T_c) and the superfluid density placed this material on the universal scaling for the cuprate materials, albeit in a region associated with Josephson coupling.²⁸ In contrast, the inferred superfluid density of the metallic (superconducting) inclusions falls on the same scaling line, but in a region associated with coherent transport and conventional superconductivity.

II. METHOD

There are two general theories of an effective medium. The first is the Maxwell Garnet dielectric function, which

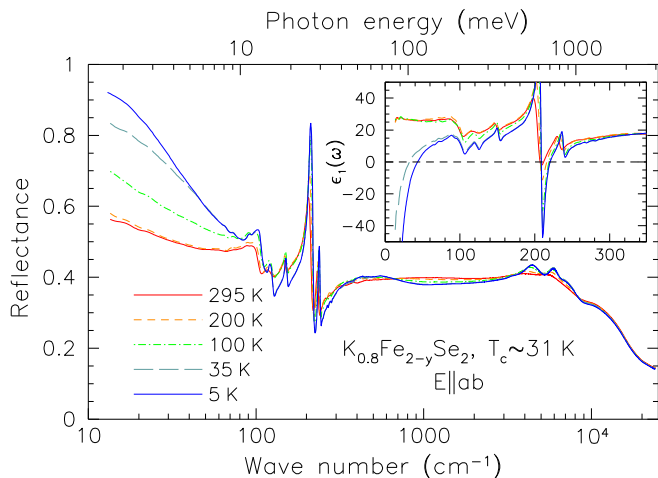


FIG. 1. The absolute reflectance over a wide frequency range for a cleaved single crystal of $\text{K}_{0.8}\text{Fe}_{2-y}\text{Se}_2$ for light polarized in the a - b planes at several temperatures above and below T_c . Inset: The temperature dependence of the real part of the dielectric function in the far-infrared region.

considers a dilute system of inclusions. A difficulty with this approach is that it is asymmetric with respect to the inclusions and the matrix. The second is the Bruggeman effective medium approximation (EMA) which is symmetric with respect to the inclusions and the matrix and is not restricted to any particular range of concentrations. Another advantage of the EMA dielectric function is that it correctly predicts the percolation threshold for spherical grains.³²

Because the metallic inclusions may represent a large volume of the sample,²⁵ we have chosen the Bruggeman EMA dielectric function. For inclusions with complex dielectric function $\tilde{\epsilon}_a$ with a volume fraction f in a matrix $\tilde{\epsilon}_b$, the EMA dielectric function $\tilde{\epsilon}$ is the root of the quadratic expression^{29–32}

$$f \frac{\tilde{\epsilon}_a - \tilde{\epsilon}}{\tilde{\epsilon}_a + \phi_c \tilde{\epsilon}} + (1 - f) \frac{\tilde{\epsilon}_b - \tilde{\epsilon}}{\tilde{\epsilon}_b + \phi_c \tilde{\epsilon}} = 0 \quad (1)$$

where the physical solution is the one that has $\text{Im}(\tilde{\epsilon}) > 0$. Here $\phi_c = (1 - g_c)/g_c$, where g_c is the depolarization factor for a spheroid

$$g_c = \frac{1 - e_c^2}{e_c^2} \left[\frac{1}{e_c} \tanh^{-1}(e_c) - 1 \right]. \quad (2)$$

For a spheroid with figure axis length c and transverse axis length a , the eccentricity of a spheroid is $e_c = \sqrt{1 - a^2/c^2}$. The EMA dielectric function is fit to the reflectance using a non-linear least squares approach; the reflectance is chosen because it is a combination of the both the real and imaginary parts of the dielectric function, as opposed to the real part of the conductivity which depends only on the imaginary part of $\tilde{\epsilon}$. The temperature dependence of the reflectance for light polarized in the planes of a single crystal of $\text{K}_{0.8}\text{Fe}_{2-y}\text{Se}_2$ with $T_c = 31$ K was determined in a previous study²⁸

and is reproduced in Fig. 1, with the real part of the dielectric function shown in the inset. Despite being a volume-averaged measurement, at low temperature the real part of the dielectric function falls below zero at low frequency, indicating a weakly metallic state. The inclusions are assumed to be metallic in the normal state (superconducting below T_c), with a complex dielectric function that may be described by a simple Drude model

$$\tilde{\epsilon}_a(\omega) = \epsilon_\infty - \frac{\omega_{p,D}^2}{\omega^2 + i\omega/\tau_D} \quad (3)$$

where ϵ_∞ is the real part of the dielectric function at high frequency, $\omega_{p,D}^2 = 4\pi n e^2/m^*$ and $1/\tau_D$ are the square of the plasma frequency and scattering rate for the delocalized (Drude) carriers, respectively, and m^* is an effective mass. The matrix is assumed to be insulating with a complex dielectric function consisting only of Lorentz oscillators

$$\tilde{\epsilon}_b(\omega) = \epsilon_\infty + \sum_j \frac{\Omega_j^2}{\omega_j^2 - \omega^2 - i\omega\gamma_j}, \quad (4)$$

where ω_j , γ_j and Ω_j are the position, width, and oscillator strength of the j th vibration. In addition to $\omega_{p,D}$ and $1/\tau_D$ in $\tilde{\epsilon}_a$, and the stronger oscillators in $\tilde{\epsilon}_b$, f and ϕ_c are both allowed to vary; ϵ_∞ is also fit, but is assumed to be the same in both $\tilde{\epsilon}_a$ and $\tilde{\epsilon}_b$. (It should be noted that in a metallic system the optical properties at low frequency are largely independent of ϵ_∞ .) From the EMA dielectric function, at normal incidence $\tilde{r} = (\sqrt{\tilde{\epsilon}} - 1)/(\sqrt{\tilde{\epsilon}} + 1)$ and $R = \tilde{r}\tilde{r}^*$. The complex conductivity is $\tilde{\sigma}(\omega) = \sigma_1 + i\sigma_2 = -i\omega[\tilde{\epsilon}(\omega) - \epsilon_\infty]/4\pi$.

The results of the non-linear least squares fits of the EMA dielectric function to the normal-state reflectance at 200, 100 and 35 K is shown in Fig. 2, as well as a comparison of the experimentally-determined optical conductivity with the calculated EMA result; the agreement with experiment is excellent. It has been previously remarked that the quality of the EMA fits is contingent on the size of the metallic inclusions being much smaller than the wavelength of the radiation in the solid.²⁵ Given the average index of refraction $n \simeq 4$ in this material²⁸ and frequency interval of the fit, a very rough value of the size of the inclusions is that they are no larger than about a micron, which is in good agreement with other estimates.^{25,42}

III. RESULTS AND DISCUSSION

A. Volume fraction

The EMA fit to the reflectance at 35 K is shown in Fig. 2(a) with the comparison to the conductivity shown in the inset; the fitted parameters are $f \simeq 0.11$ and $\phi_c \simeq 30$ with the Drude parameters $\omega_{p,D} \simeq 1320 \text{ cm}^{-1}$ and $1/\tau_D \simeq 57 \text{ cm}^{-1}$. For the fits at 100 and 200 K shown

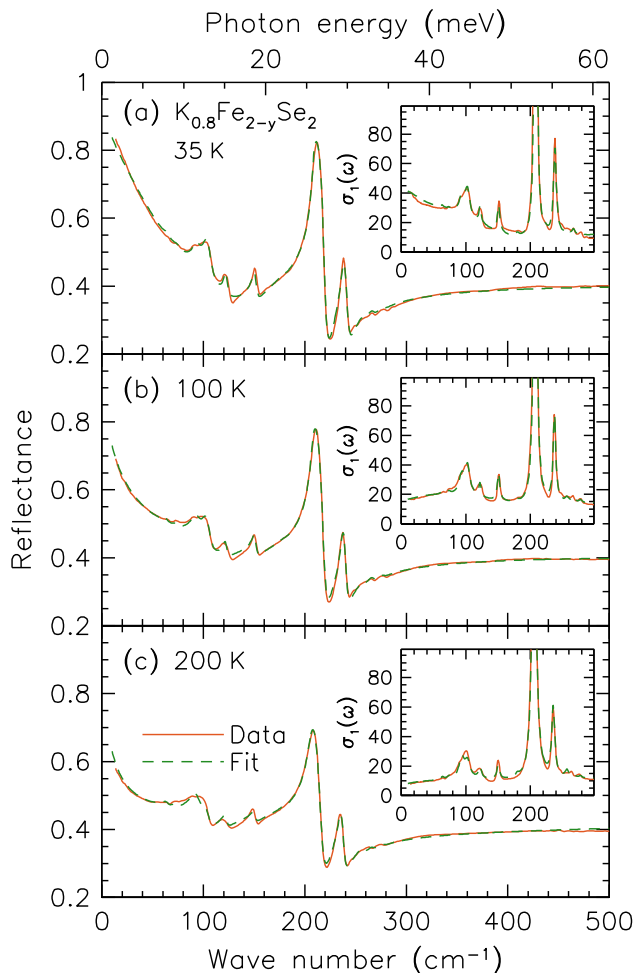


FIG. 2. The results of the fits of the Bruggeman EMA dielectric function to the reflectance of $K_{0.8}Fe_{2-y}Se_2$ in the far-infrared region for light polarized in the a - b planes at (a) 35 K, (b) 100 K and (c) 200 K. Inset: The fit compared to the real part of the conductivity.

in Figs. 2(b) and (c), f , ϕ_c and $\omega_{p,D}$ are fixed and the scattering rate is allowed to vary, returning $1/\tau_D \simeq 126$ and 144 cm^{-1} , respectively. (Note that the optical properties at 200 and 295 K are almost identical.²⁸) The estimate that only about 10% of the sample is conducting (superconducting) is in good agreement with recent Mössbauer,¹⁷ NMR,²⁰ and bulk muon-spin rotation (μ SR)^{23–25} studies. The strengths of the fitted Lorentz oscillators are nearly identical to the previously determined values,²⁸ with $\epsilon_\infty \simeq 4.6$ (the same value used for the metallic inclusions). Given that the insulating matrix accounts for about 90% of the sample volume, it is not surprising that the vibrational parameters should remain essentially unchanged. Previous Drude-Lorentz fits to the volume-averaged optical conductivity at 35 K yielded $\omega_{p,D}^{vol} \simeq 430 \text{ cm}^{-1}$ and $1/\tau_D^{vol} \simeq 70 \text{ cm}^{-1}$;²⁸ this result is consistent with the typically low values of $\omega_{p,D}^{vol}$ observed in these materials.^{25–27} If we attribute this average plasma frequency to the fraction f of the sample

that is metallic, then

$$\frac{\omega_{p,D}}{\omega_{p,D}^{vol}} = \frac{1}{\sqrt{f}}. \quad (5)$$

For $f \simeq 0.11$, $\omega_{p,D} = \omega_{p,D}^{vol}/\sqrt{f} \simeq 1300 \text{ cm}^{-1}$; this value is almost identical to the fitted EMA value of $\omega_{p,D} \simeq 1320 \text{ cm}^{-1}$. The value for $\omega_{p,D}$ is still rather small when compared with values of $\omega_{p,D} \simeq 7000 - 14000 \text{ cm}^{-1}$ observed in other iron-based superconductors.^{33–39} Indeed, for $\omega_{p,D}$ to rival these values would require a volume fraction of less than 1%. Setting the fraction of metallic inclusions to $f = 0.005$ yields the EMA fitted value of $\omega_{p,D} \simeq 6620 \text{ cm}^{-1}$ (close to the value of 6080 cm^{-1} based on the volume average), and $1/\tau_D \simeq 38 \text{ cm}^{-1}$; however, the fitted value $\phi_c \gtrsim 200$ is quite large and the overall quality of the fit has decreased significantly. In either case, the temperature dependence of the volume-averaged conductivity was originally described as incoherent at room temperature with a large scattering rate that decreases rapidly with temperature resulting in a crossover to coherent behavior at low temperature. However, assuming $f \simeq 0.1$, the EMA values for $1/\tau_D$ suggest that the transport in the metallic regions is always coherent.

The value for $\phi_c \simeq 30$ yields the rather small value for the depolarization factor $g_c \simeq 0.032$ which corresponds to an eccentricity $e_o \simeq 0.93$ for an oblate spheroid or $e_c \simeq 0.99$ in a prolate spheroid; both cases correspond to highly distorted shapes. This condition becomes even more severe for larger values of ϕ_c . The layered nature of these materials^{43–45} and the anisotropic transport properties⁴⁶ suggests that these distorted shapes overlap or are joined through weak links to form a conducting pathways through the solid, resulting in a predominantly two-dimensional filamentary network, or a superconducting aerogel.^{21,41}

In this approach we have assumed that the highly-distorted inclusions overlap to some degree. However, it might also be possible that a large number of inclusions may be isolated, in which case for spherical particles with $\epsilon_\infty = 1$ for both the inclusions and the matrix, the effective dielectric function would experience a resonance at $\omega_0 = \omega_{p,D} \sqrt{(1-f)/3} \simeq 720 \text{ cm}^{-1}$ (Maxwell Garnet theory³²). However, the values $\epsilon_\infty = 4.6$ and $\phi_c \simeq 30$ dramatically lower this resonance, $\omega_0 \lesssim 100 \text{ cm}^{-1}$. The absence of such a feature in our results suggests that either a continuous distribution of shapes has rendered this feature too broad and weak to be observed, or that there are simply very few isolated inclusions.

B. Energy scales

In the iron-chalcogenide superconductors, the energy scales for the isotropic superconducting energy gaps that are observed in angle-resolved photoemission spectroscopy (ARPES) to open on the hole and electron pockets below T_c are usually in excellent agreement with the

optical gaps observed in the conductivity that develop in the superconducting state.^{39,47} However, these two energy scales appear to be very different in $\text{K}_{0.8}\text{Fe}_{2-y}\text{Se}_2$. While the ARPES estimate of the isotropic optical gap is $2\Delta \simeq 16 - 20 \text{ meV}$ ($\simeq 130 - 160 \text{ cm}^{-1}$),⁴⁻⁶ the reflectance (and the conductivity) indicates that the energy scale associated with the superconductivity in this material is much smaller, $\simeq 8 \text{ meV}$. This difference originates from the inhomogeneous nature of this material. ARPES is insensitive to the insulating matrix and directly probes the formation of a superconducting gap in the metallic (superconducting) inclusions, while the optical properties are a volume-averaging technique which will be sensitive to the Josephson coupling between the superconducting regions. In such a Josephson coupled system, changes in the reflectance (for instance) will occur not at 2Δ but at the renormalized superconducting plasma frequency, $\tilde{\omega}_{p,S} = \omega_{p,S}/\sqrt{\epsilon_{\text{FIR}}}$, or at the average value for a distribution of frequencies.²⁷ Given $\omega_{p,S} \simeq 220 \text{ cm}^{-1}$ and $\epsilon_{\text{FIR}} \simeq 18$ at 50 meV (inset of Fig. 1), then $\tilde{\omega}_{p,S} \simeq 52 \text{ cm}^{-1}$ or $\simeq 6.5 \text{ meV}$, which is very close to the changes in the optical properties observed to occur below $\simeq 8 \text{ meV}$. Thus, due to the inhomogeneous nature of this superconductor, optics and ARPES probe two different quantities, $\tilde{\omega}_{p,S}$ and Δ , respectively.

C. Parameter scaling

It has been pointed out that a number of the iron-based superconductors⁴⁸ fall on the scaling relation initially observed for the cuprate superconductors,⁴⁹⁻⁵¹ $\rho_{s0}/8 \simeq 4.4 \sigma_{dc} T_c$, where the superfluid density is $\rho_{s0} \equiv \omega_{p,S}^2$. In our previous optical study of $\text{K}_{0.8}\text{Fe}_{2-y}\text{Se}_2$ the volume averaged value for the superconducting plasma frequency was determined to be $\omega_{p,S}^{\text{vol}} \simeq 220 \text{ cm}^{-1}$ (Ref. 28). While this value is quite small, this material does indeed fall on the universal scaling line; however, it does so in a region associated with the response along the c axis in the cuprates where the superconductivity is due to Josephson coupling between the copper-oxygen planes. From this it was concluded that the superconductivity was due to the Josephson coupling of discrete superconducting regions and that the material constituted a Josephson phase.^{52,53}

The superconducting plasma frequency for the inclusions with $f = 0.1$ may be estimated below T_c using $\omega_{p,S} = \omega_{p,S}^{\text{vol}}/\sqrt{f} \simeq 700 \text{ cm}^{-1}$, which corresponds to an effective penetration depth of $\lambda_{eff} \simeq 2.2 \mu\text{m}$. We note that the EMA model yields a lower value for the normal-state scattering rate $1/\tau_D \simeq 57 \text{ cm}^{-1}$ at 35 K than the volume average, $1/\tau_D^{\text{vol}} \simeq 70 \text{ cm}^{-1}$. This smaller value for $1/\tau_D$ results in the condition $1/\tau_D < 2\Delta$. This would normally imply that more spectral weight (the area under the conductivity curve) associated with the free carriers lies in the gap and thus more spectral weight should be transferred to the condensate.⁵⁰ In the volume average case, only about 25% of the free carriers collapse into

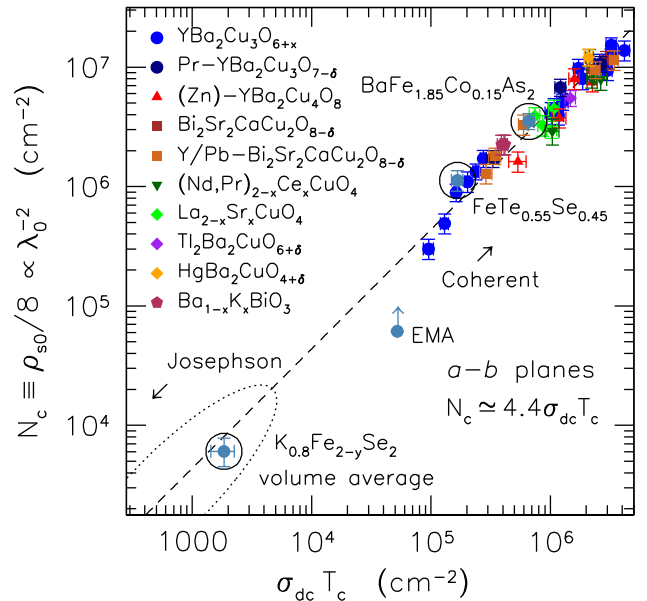


FIG. 3. The log-log plot of the spectral weight of the superfluid density $N_c \equiv \rho_{s0}/8$ vs $\sigma_{dc} T_c$ in the a - b planes for a variety of cuprate superconductors, as well as several iron-based superconductors, compared with the volume average and EMA results for $\text{K}_{0.8}\text{Fe}_{2-y}\text{Se}_2$. The dashed line corresponds to the general result for the cuprates $\rho_{s0}/8 \simeq 4.4\sigma_{dc} T_c$, while the dotted line denotes the region of the scaling relation typically associated with Josephson coupling along the c axis. While the volume average result signalled a Josephson phase, the EMA result now lies very close to the coherent regime.

the condensate; the EMA result implies that the estimate of $\omega_{p,S} \simeq 700 \text{ cm}^{-1}$ likely represents a minimum value. However, the issue of the scattering rate itself is somewhat complicated. Despite the fact that this material has only electron pockets, it has been proposed that the scattering rate is anisotropic;⁵⁴ this has resulted in some workers adopting a two-component model with large and small scattering rates.^{25,26} In the EMA fits used here, only a single component has been employed. Therefore, if there is in fact a distribution of scattering rates, the fitted EMA value will represent an average value. As a result, there is some uncertainty attached to the value of $1/\tau_D$. With this caveat in place, the EMA fit to the reflectance just above T_c at 35 K may be used to estimate the dc conductivity of the metallic inclusions, $\sigma_{dc} = \omega_{p,D}^2 \tau_D / 60 \simeq 510 \Omega^{-1} \text{cm}^{-1}$. The values for $\omega_{p,S}$ and σ_{dc} once again place this material close to the scaling line, but now the material falls very close to the other iron-chalcogenide superconductors, as shown in Fig. 3.

While $\omega_{p,S}$ is significantly larger than the volume-averaged value, it is still almost an order of magnitude smaller than μSR ^{23,25} and NMR⁵⁵ estimates, although adopting a smaller value for the volume fraction f negates this difference. On the other hand, the value of $\lambda_{eff} \simeq 2.2 \mu\text{m}$ in the superconducting regions of $\text{K}_{0.8}\text{Fe}_{2-y}\text{Se}_2$ is in surprisingly good agreement with the in-plane optical estimate of $\lambda \simeq 2 \mu\text{m}$ in $\text{Rb}_2\text{Fe}_4\text{Se}_5$

using an EMA approach.²⁴

IV. CONCLUSIONS

The complex optical properties of $\text{K}_{0.8}\text{Fe}_{2-y}\text{Se}_2$ in the normal state have been modeled using the Bruggeman EMA. The volume fraction of the metallic inclusion is estimated to be $f \simeq 0.1$; however, the EMA can only be successfully fit to the data if the inclusions are highly distorted, suggesting a filamentary network of conducting regions joined through weak links. The plasma frequency in the metallic inclusions is therefore considerably larger than the volume-averaged value, $\omega_{p,D} > \omega_{p,D}^{vol}$; however, $\omega_{p,D} \simeq 1320 \text{ cm}^{-1}$ is still much smaller than the values for the plasma frequency observed in other (homogeneous) iron-based superconductors, as is the estimate of $\omega_{p,S} \simeq 700 \text{ cm}^{-1}$ (unless volume fractions of less than 1% are considered). The reasonably small values for $1/\tau_D \simeq 60 - 140 \text{ cm}^{-1}$ returned by the EMA fits sug-

gests that the transport in the metallic regions is always coherent, and that there is no crossover from incoherent behavior as the temperature is lowered. The inferred $\sigma_{dc} \simeq 510 \text{ } \Omega^{-1}\text{cm}^{-1}$ just above T_c and the estimated lower bound of $\rho_{s0} \simeq 4.9 \times 10^5 \text{ cm}^{-2}$ for the metallic (superconducting) inclusions shifts this material away from the region on the scaling line associated with Josephson coupling to a region where the majority of (homogeneous) iron-based superconductors are observed to lie.

ACKNOWLEDGMENTS

We would like to thank A. Akrap, G. L. Carr, A. Charnukha, and D. van der Marel for useful discussions. Research supported by the U.S. Department of Energy, Office of Basic Energy Sciences, Division of Materials Sciences and Engineering under Contract No. DE-AC02-98CH10886. Z. X. and J. W. are supported by the Center for Emergent Superconductivity, an Energy Frontier Research Consortium supported by the Office of Basic Energy Science of the Department of Energy

-
- * homes@bnl.gov
- ¹ D. C. Johnston, *Adv. Phys.* **59**, 803 (2010).
 - ² S. Raghu, X.-L. Qi, C.-X. Liu, D. J. Scalapino, and S.-C. Zhang, *Phys. Rev. B* **77**, 220503(R) (2008).
 - ³ A. Chubukov, *Ann. Rev. Condens. Matt. Phys.* **3**, 57 (2012).
 - ⁴ T. Qian, X.-P. Wang, W.-C. Jin, P. Zhang, P. Richard, G. Xu, X. Dai, Z. Fang, J.-G. Guo, X.-L. Chen, and H. Ding, *Phys. Rev. Lett.* **106**, 187001 (2011).
 - ⁵ X.-P. Wang, T. Qian, P. Richard, P. Zhang, J. Dong, H.-D. Wang, C.-H. Dong, M.-H. Fang, and H. Ding, *EPL* **93**, 57001 (2011).
 - ⁶ Y. Zhang, L. X. Yang, M. Xu, Z. R. Ye, F. Chen, C. He, H. C. Xu, J. Jiang, B. P. Xie, J. J. Ying, X. F. Wang, X. H. Chen, J. P. Hu, M. Matsunami, S. Kimura, and D. L. Feng, *Nature Mater.* **10**, 273277 (2011).
 - ⁷ J. Guo, S. Jin, G. Wang, S. Wang, K. Zhu, T. Zhou, M. He, and X. Chen, *Phys. Rev. B* **82**, 180520(R) (2010).
 - ⁸ H. Chen, Y. Ren, Y. Qiu, W. Bao, R. H. Liu, G. Wu, T. Wu, Y. L. Xie, X. F. Wang, Q. Huang, and X. H. Chen, *EPL* **85**, 17006 (2009).
 - ⁹ T. Sato, K. Nakayama, Y. Sekiba, P. Richard, Y.-M. Xu, S. Souma, T. Takahashi, G. F. Chen, J. L. Luo, N. L. Wang, and H. Ding, *Phys. Rev. Lett.* **103**, 047002 (2009).
 - ¹⁰ F. Wang, F. Yang, M. Gao, Z.-Y. Lu, T. Xiang, and D.-H. Lee, *EPL* **93**, 57003 (2011).
 - ¹¹ Z. Wang, Y. J. Song, H. L. Shi, Z. W. Wang, Z. Chen, H. F. Tian, G. F. Chen, J. G. Guo, H. X. Yang, and J. Q. Li, *Phys. Rev. B* **83**, 140505(R) (2011).
 - ¹² B. Shen, B. Zeng, G. F. Chen, J. B. He2, D. M. Wang, H. Yang, and H. H. Wen, *EPL* **96**, 37010 (2011).
 - ¹³ A. Ricci, N. Poccia, G. Campi, B. Joseph, G. Arrighetti, L. Barba, M. Reynolds, M. Burghammer, H. Takeya, Y. Mizuguchi, Y. Takano, M. Colapietro, N. L. Saini, and A. Bianconi, *Phys. Rev. B* **84**, 060511(R) (2011).
 - ¹⁴ A. Ricci, N. Poccia, B. Joseph, G. Arrighetti, L. Barba, J. Plaisier, G. Campi, Y. Mizuguchi, H. Takeya, Y. Takano, N. L. Saini, and A. Bianconi, *Supercond. Sci. Technol.* **24**, 082002 (2011).
 - ¹⁵ R. H. Liu, X. G. Luo, M. Zhang, A. F. Wang, J. J. Ying, X. F. Wang, Y. J. Yan, Z. J. Xiang, P. Cheng, G. J. Ye, Z. Y. Li, and X. H. Chen, *EPL* **94**, 27008 (2011).
 - ¹⁶ A. M. Zhang, J. H. Xiao, Y. S. Li, J. B. He, D. M. Wang, G. F. Chen, B. Normand, Q. M. Zhang, and T. Xiang, *Phys. Rev. B* **85**, 214508 (2012).
 - ¹⁷ V. Ksenofontov, G. Wortmann, S. A. Medvedev, V. Tsurkan, J. Deisenhofer, A. Loidl, and C. Felser, *Phys. Rev. B* **84**, 180508 (2011).
 - ¹⁸ L. Simonelli, N. L. Saini, M. M. Sala, Y. Mizuguchi, Y. Takano, H. Takeya, T. Mizokawa, and G. Monaco, *Phys. Rev. B* **85**, 224510 (2012).
 - ¹⁹ W. Li, H. Ding, P. Deng, K. Chang, C. Song, K. He, L. Wang, X. Ma, J.-P. Hu, X. Chen, and Q.-K. Xue, *Nat. Phys.* **8**, 126 (2012).
 - ²⁰ Y. Texier, J. Deisenhofer, V. Tsurkan, A. Loidl, D. S. Inosov, G. Friemel, and J. Bobroff, *Phys. Rev. Lett.* **108**, 237002 (2012).
 - ²¹ Z. W. Wang, Z. Wang, Y. J. Song, C. Ma, H. L. Shi, Z. Chen, H. F. Tian, H. X. Yang, G. F. Chen, and J. Q. Li, (2012), arXiv:1204.4542 (unpublished).
 - ²² W. Li, H. Ding, Z. Li, P. Deng, K. Chang, K. He, S. Ji, L. Wang, X. Ma, J.-P. Hu, X. Chen, and Q.-K. Xue, *Phys. Rev. Lett.* **109**, 057003 (2012).
 - ²³ R. Shermadini, A. Krzton-Maziopa, M. Bendele, Z. Khasanov, H. Luetkens, K. Conder, E. Pomjakushina, S. Weyeneth, V. Pomjakushin, O. Bossen, and A. Amato, *Phys. Rev. Lett.* **106**, 117602 (2011).
 - ²⁴ A. Charnukha, A. Cvitkovic, T. Prokscha, D. Pröpper, N. Ocelic, A. Suter, Z. Salman, E. Morenzoni, J. Deisenhofer, V. Tsurkan, A. Loidl, B. Keimer, and A. V. Boris,

- Phys. Rev. Lett. **109**, 017003 (2012).
- 25 C. N. Wang, P. Marsik, R. Schuster, A. Dubroka, M. Rössle, C. Niedermayer, G. D. Varma, A. F. Wang, X. H. Chen, T. Wolf, and C. Bernhard, Phys. Rev. B **85**, 214503 (2012).
 - 26 A. Charnukha, J. Deisenhofer, D. Pröpper, M. Schmidt, Z. Wang, Y. Goncharov, A. N. Yaresko, V. Tsurkan, B. Keimer, A. Loidl, and A. V. Boris, Phys. Rev. B **85**, 100504(R) (2012).
 - 27 R. H. Yuan, T. Dong, Y. J. Song, G. F. Chen, J. P. Hu, J. Q. Li, and N. L. Wang, Sci. Rep. **2**, 221 (2012).
 - 28 C. C. Homes, Z. J. Xu, J. S. Wen, and G. D. Gu, Phys. Rev. B **85**, 180510(R) (2012).
 - 29 D. Stroud, Phys. Rev. B **12**, 3368 (1975).
 - 30 D. Walker and K. Scharnberg, Phys. Rev. B **42**, 2211 (1990).
 - 31 C. Brosseau, J. App. Phys. **91**, 3197 (2002).
 - 32 G. L. Carr, S. Perkowitz, and D. B. Tanner, “Far-infrared properties of inhomogeneous materials,” in *Infrared and Millimeter Waves*, Vol. 13, edited by K. J. Button (Academic Press, Orlando, FL, 1986) pp. 171 – 263.
 - 33 J. Yang, D. Hüvonen, U. Nagel, T. Rõõm, N. Ni, P. C. Canfield, S. L. Bud’ko, J. P. Carbotte, and T. Timusk, Phys. Rev. Lett. **102**, 187003 (2009).
 - 34 D. Wu, N. Barišić, N. Drichko, S. Kaiser, A. Faridian, M. Dressel, S. Jiang, Z. Ren, L. J. Li, G. H. Cao, Z. A. Xu, H. S. Jeevan, and P. Gegenwart, Phys. Rev. B **79**, 155103 (2009).
 - 35 W. Hu, Q. Zhang, and N. Wang, Physica C **469**, 545 (2009).
 - 36 R. P. S. M. Lobo, Y. M. Dai, U. Nagel, T. Rõõm, J. P. Carbotte, T. Timusk, A. Forget, and D. Colson, Phys. Rev. B **82**, 100506(R) (2010).
 - 37 J. J. Tu, J. Li, W. Liu, A. Punnoose, Y. Gong, Y. H. Ren, L. J. Li, G. H. Cao, Z. A. Xu, and C. C. Homes, Phys. Rev. B **82**, 174509 (2010).
 - 38 N. Barišić, D. Wu, M. Dressel, L. J. Li, G. H. Cao, and Z. A. Xu, Phys. Rev. B **82**, 054518 (2010).
 - 39 C. C. Homes, A. Akrap, J. S. Wen, Z. J. Xu, Z. W. Lin, Q. Li, and G. D. Gu, Phys. Rev. B **81**, 180508(R) (2010).
 - 40 C. C. Homes, A. Akrap, J. Wen, Z. Xu, Z. W. Lin, Q. Li, and G. Gu, J. Phys. Chem. Solids **72**, 505 (2011).
 - 41 R. Hu, E. D. Mun, D. H. Ryan, K. Cho, H. Kim, H. Hodovanets, W. E. Straszheim, M. A. Tanatar, R. Prozorov, W. N. Rowan-Weetaluktuk, J. M. Cadogan, M. M. Altarawneh, C. H. Mielke, V. S. Zapf, S. L. Bud’ko, and P. C. Canfield, (2012), arXiv:1201.0953 (unpublished).
 - 42 S. C. Speller, T. B. Britton, G. M. Hughes, A. Krzton-Maziopa, E. Pomjakushina, K. Conder, A. T. Boothroyd, and C. R. M. Grovenor, Superconductor Science and Technology **25**, 084023 (2012).
 - 43 W. Bao, Q.-Z. Huang, G.-F. Chen, M. A. Green, D.-M. Wang, J.-B. He, and Y.-M. Qiu, Chin. Phys. Lett. **28**, 086104 (2011).
 - 44 J. Bacsá, A. Y. Ganin, Y. Takabayashi, K. E. Christensen, K. Prassides, M. J. Rosseinsky, and J. B. Claridge, Chem. Sci. **2**, 1054 (2011).
 - 45 P. Zavalij, W. Bao, X. F. Wang, J. J. Ying, X. H. Chen, D. M. Wang, J. B. He, X. Q. Wang, G. F. Chen, P.-Y. Hsieh, Q. Huang, and M. A. Green, Phys. Rev. B **83**, 132509 (2011).
 - 46 H.-D. Wang, C.-H. Dong, Z.-J. Li, Q.-H. Mao, S.-S. Zhu, C.-M. Feng, H. Q. Yuan, and M.-H. Fang, EPL **93**, 47004 (2011).
 - 47 H. Miao, P. Richard, Y. Tanaka, K. Nakayama, T. Qian, K. Umezawa, T. Sato, Y.-M. Xu, Y. B. Shi, N. Xu, X.-P. Wang, P. Zhang, H.-B. Yang, Z.-J. Xu, J. S. Wen, G.-D. Gu, X. Dai, J.-P. Hu, T. Takahashi, and H. Ding, Phys. Rev. B **85**, 094506 (2012).
 - 48 D. Wu, N. Barišić, N. Drichko, P. Kallina, A. Faridian, B. Gorshunov, M. Dressel, L. J. Li, X. Lin, G. H. Cao, and Z. A. Xu, Physica C **470**, S399 (2010).
 - 49 C. C. Homes, S. V. Dordevic, M. Strongin, D. A. Bonn, R. Liang, W. N. Hardy, S. Komiyá, Y. Ando, G. Yu, N. Kaneko, X. Zhao, M. Greven, D. N. Basov, and T. Timusk, Nature (London) **430**, 539 (2004).
 - 50 C. C. Homes, S. V. Dordevic, T. Valla, and M. Strongin, Phys. Rev. B **72**, 134517 (2005).
 - 51 C. C. Homes, S. V. Dordevic, D. A. Bonn, R. Liang, W. N. Hardy, and T. Timusk, Phys. Rev. B **71**, 184515 (2005).
 - 52 Y. Imry, M. Strongin, and C. Homes, Physica C **468**, 288 (2008).
 - 53 Y. Imry, M. Strongin, and C. C. Homes, Phys. Rev. Lett. **109**, 067003 (2012).
 - 54 A. F. Kemper, M. M. Korshunov, T. P. Devereaux, J. N. Fry, H.-P. Cheng, and P. J. Hirschfeld, Phys. Rev. B **83**, 184516 (2011).
 - 55 D. A. Torchetti, M. Fu, D. C. Christensen, K. J. Nelson, T. Imai, H. C. Lei, and C. Petrovic, Phys. Rev. B **83**, 104508 (2011).